

Origin of hysteresis in shock wave reflection

Yan-Chao Hu, Zhi-Gong Tang, Yan-Guang Yang, Wen-Feng Zhou, Zhao-Hu Qin
China Aerodynamics Research and Development Center;
Peking University
 (Dated: January 24, 2022)

We report the mechanism of the hysteresis in the transition between Regular and Mach reflections. A new discovery is that, the hysteresis loop is in fact the projection of a higher dimensional path, i.e. the valley lines in the surface of dissipation, of which minimal values correspond to stable reflection configurations. Since the saddle-nodes bifurcate the valleys of the surface, they are actually the transition points of the two reflections. Furthermore, the predicted reflection configurations agree well with the experimental and numerical results, which is a validation of this theory.

Hysteresis is a general property of systems with two or more possible steady states, where hysteresis loops always emerge as external parameters vary continuously. A canonical example is the system described by the ferromagnetism theory [1], where cyclical variation of the magnetic field intensity H induces a hysteresis loop of the magnetization κ . H is the external parameter of the system, and κ is the order parameter, proposed by Landau [2], manifesting the ferromagnet state. Other systems such as liquid–solid phase transitions [3, 4], laminar-turbulent transitions [5–8] and Bose–Einstein condensation [9–12] all possess this property.

In shock wave reflections, which are ubiquitous in aerospace engineering, hystereses also exist in the transition between regular reflection (RR) and Mach reflection (MR), which two different configurations were first observed by Mach [13] in 1878, as shown in figure 1(a), where RR corresponds to state 1, 2 and MR corresponds to state 3, 4, each of which has a segment of normal shock waves named Mach stem. More than half a century after that, von Neumann [14] proposed two critical deflection angles, the detachment condition θ_w^D and von Neumann condition θ_w^N , for the $RR \rightleftharpoons MR$ transition. As shown in figure 1(b) and 1(c), only RRs exist if the wedge angle $\theta_w < \theta_w^N$ and only MRs exist when $\theta_w > \theta_w^D$. However, in the intermediate range $\theta_w^N \leq \theta_w \leq \theta_w^D$, both stable RRs and MRs are theoretically possible, which makes range- $[\theta_w^N, \theta_w^D]$ referred to as a dual-solution domain. Based on this fact, Hornung [15] hypothesized that hystereses exist in $RR \rightleftharpoons MR$ transitions, which was verified both experimentally [16] and numerically [17] later on, and re-initiated the researchers interest in the $RR \rightleftharpoons MR$ transition, particularly, the hysteresis process [18–20]. Figure 1(a) shows flow configurations of hysteresis induced by θ_w variation corresponding to the states in figure 1(b). As θ_w varies continuously from 20° (in the overall RR domain) to 24° (in the dual-solution domain), the configuration maintains stable RR (from state 1 to 2). However, if θ_w varies from 28° (in the overall MR domain) back to 24° , it will maintain stable MR (from state 3 to 4). It is noted that at $\theta_w = 24^\circ$, either stable RR or MR appearing depends on the evolution history. Obviously, state $1 \rightarrow 2 \rightarrow 3 \rightarrow 4 \rightarrow 1$ constitutes a hysteresis loop. Although forty years has passed since the hysteresis was put forward [15], the mechanism behind this complex phenomenon is still not clear.

In this letter, the least-action principle is used to reveal the

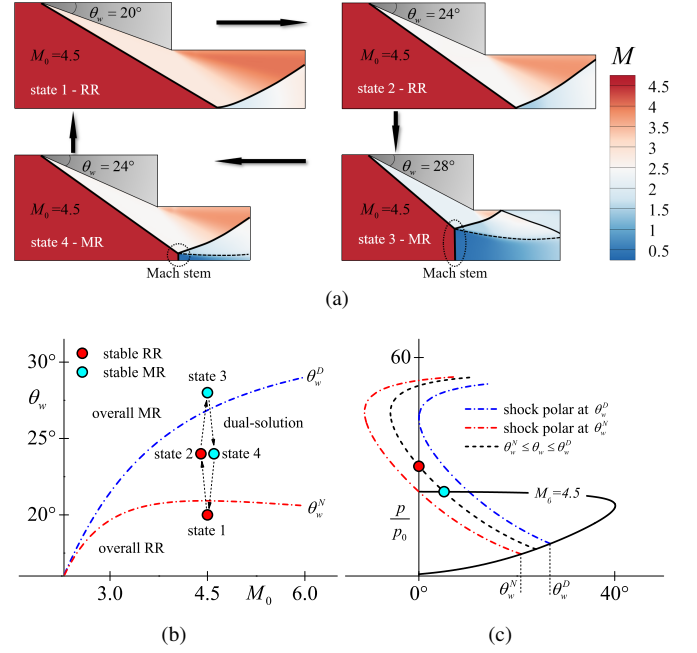


FIG. 1: (a) distributions of local Mach number M of state 1,2,3 and 4 obtained by numerical computation at $M_0 = 4.5$; (b) θ_w^D and θ_w^N varying with the inflow Mach number M_0 , and the hysteresis loop (state 1, 2, 3 and 4) induced by θ_w variation at $M_0 = 4.5$; (c) shock polars at θ_w^D , θ_w^N and θ_w at $M_0 = 4.5$, where θ_w is in the dual-solution domain.

essence of hysteresis in the $RR \rightleftharpoons MR$ transition, i.e. how the reflection depends on its evolution history and where the transition happens.

First, we will introduce the reflection configuration. As shown in figure 2(a), for a given wedge angle θ_w in the dual-solution domain, a general reflection configuration is composed of (i) an incident shock wave AT , (ii) a strong shock wave called the Mach stem TG with height h_m ($h_m = 0$ corresponds to a RR and $h_m > 0$ corresponds to a MR) and (iii) a reflected shock wave including a straight segment TB , a curved segment BC and another straight segment CD . It is notice that, in analogy with the magnetization κ manifesting the ferromagnet state in the ferromagnetism theory [1, 2], the Mach stem

height h_m also manifests the flow state in the shock wave reflection, then it is actually the order parameter of this system, and θ_w is the external parameter analogous with the magnetic field intensity H . For a MR ($h_m > 0$), a free shear layer TS exists, below which the flow can be regarded as Quasi-one-dimensional isentropic duct flow. Behind the reflected shock wave TD , the flow is expanded or weakly compressed, which can also be regarded as isentropic [21, 22].

Then we will demonstrate that the reflection flow system has the minimal dissipation. The Helmholtz-Rayleigh dissipation theorem [23–25] put forward that an incompressible viscous fluid should have the minimal dissipation if the acceleration $\mathbf{a} = \mathbf{u} \cdot \nabla \mathbf{u}$ can be derived by a potential ζ , i.e. $\mathbf{a} = \nabla \zeta$ or $\nabla \times \mathbf{a} = 0$. This theorem was extended to compressible flows by He et al [26, 27] in 1988. Mathematically, it means that the steady compressible Navier-Stokes equation:

$$\mathbf{u} \cdot \nabla \mathbf{u} = -\frac{1}{\rho} \nabla p + \mathbf{f} + \frac{1}{\rho} [\nabla(\eta\vartheta) + \nabla \cdot (2\mu\mathbf{D})] \quad (1)$$

can be derived by the variation of the dissipation. In function (1), \mathbf{u} , p , ρ , \mathbf{f} , η and μ are the velocity, pressure, density, body force, dilatation and shear viscosity of the flow, respectively. $\vartheta = \nabla \cdot \mathbf{u}$ and $\mathbf{D} = [\nabla \mathbf{u} + (\nabla \mathbf{u})^T]/2$ are the divergence and the strain-rate tensor, respectively. $\phi = \eta\vartheta^2 + 2\mu\mathbf{D} : \mathbf{D}$ is the kinetic energy dissipation [27]. We consider the total dissipation Φ in control volume V bounded by ℓ , which satisfies that V is nondeformable or the flow on mobile ℓ (if V is deformable) is nondissipative. With the constraint served by the steady continuity equation $\nabla \cdot (\rho\mathbf{u}) = 0$, the variation of Φ can be written as:

$$\delta\Phi = \delta \int_V [\phi + \lambda \nabla \cdot (\rho\mathbf{u})] dV = 0 \quad (2)$$

where λ is Lagrangian multiplier, and $L = \phi + \lambda \nabla \cdot (\rho\mathbf{u})$ is the Lagrangian. Since \mathbf{u} and ρ are the two independent variables of L , the Euler-Lagrangian equation is:

$$\frac{\delta L}{\delta \mathbf{u}} = 0 : [\nabla(\eta\vartheta) + \nabla \cdot (2\mu\mathbf{D})] + \frac{1}{2}\rho\nabla\lambda = 0 \quad (3)$$

$$\frac{\delta L}{\delta \rho} = 0 : \mathbf{u} \cdot \nabla\lambda = 0 \quad (4)$$

If a flow satisfies that (i) $\mathbf{a} = \nabla\zeta$; (ii) $\mathbf{f} = \nabla U$, i.e. the body force can be derived by a potential U ; (iii) $\nabla p/\rho = \nabla \int dp/\rho$, i.e. the flow is barotropic which is equivalent to $\nabla p \times \nabla \rho = 0$, then when λ is chosen as $\lambda = -2\left(\zeta + \int dp/\rho + U\right)$, formular (3) can be exactly rearranged to function (1), and formular (4) is the Bernoulli Integration. Therefore, a flow satisfying (i), (ii) and (iii) has the minimal dissipation.

For a flow passing through a straight shock wave, the acceleration \mathbf{a} can be decomposed into two parts relative to the shock front, i.e. the normal component a_n and tangential one a_τ (consider a 2D flow field). Since the velocity only changes perpendicularly through the shock, there must be $\partial a_n/\partial \tau = 0$ and $a_\tau = 0$, then $|\nabla \times \mathbf{a}| = \partial a_\tau/\partial n - \partial a_n/\partial \tau = 0$, which implies that condition (i) is satisfied. Additionally, the body

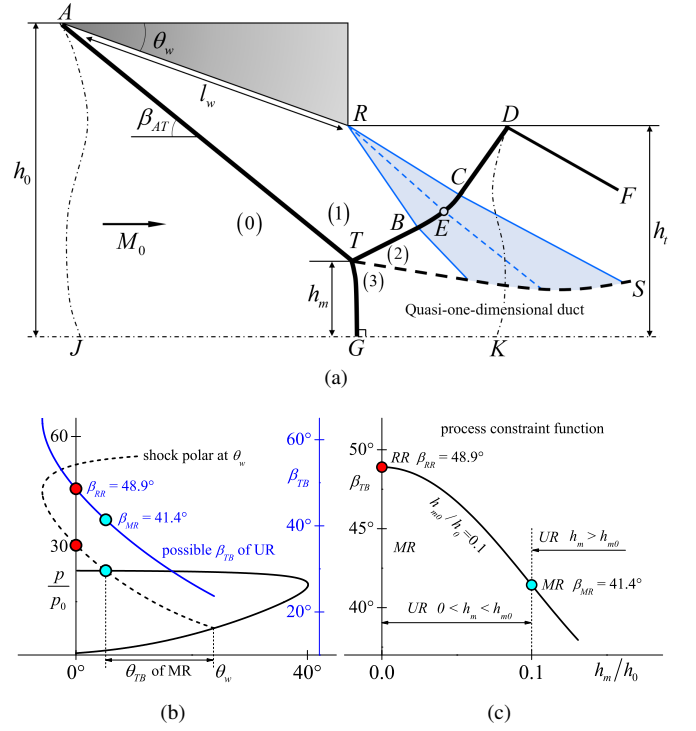


FIG. 2: (a) the illustration of a general reflection configuration with a Mach stem height h_m ; (b) possible β_{TB} of unstable reflection configurations; (c) process constraint function of β_{AT} with the order parameter h_m .

force \mathbf{f} is gravity that can be negligible, which means condition (ii) is satisfied. ∇p and $\nabla \rho$ are both perpendicular to the shock front, which implies $\nabla p \times \nabla \rho = 0$ and then condition (iii) is satisfied. Therefore, a steady flow across a straight shock wave has minimal dissipation. This is also the reason that, although both a weak and a strong oblique shock wave are theoretically possible at a same deflection angle, the observable shock wave in reality is always the weak one. Furthermore, if a shock wave is curved, its curvature radius is always infinitely great compared to its thickness, then it can also be approximated to a straight one. Therefore, if the total dissipation of a steady flow field is only contributed by shock waves, this flow should have minimal dissipation.

For the flow system shown in figure 2(a), a control volume V is chosen to enclose the reflection configuration, of which boundaries ℓ are composed of the upper wall ARD , the reflected surface JK , the inflow surface AJ and the outflow surface DK . Except shock waves, dissipation could also happen in (i) the isentropic region and (ii) the shear layer TS . For the isentropic region, the relationship of ϕ and entropy generation ds/dt is that $\phi = \mathcal{T} ds/dt$ [27], where \mathcal{T} is the flow temperature, then "isentropic" $ds/dt = 0$ means "nondissipative" $\phi = 0$. For the shear layer, the dissipation induced by (ii) TS and a shock wave are $\int_{\varepsilon_\delta} \phi dx \sim \mu \Delta u^2/\varepsilon_\delta$ and $\int_\varepsilon \phi dx \sim \mu \Delta u^2/\varepsilon$, respectively, where ε_δ and ε are the thickness of TS and the shock wave, respectively, and dx is the

normal infinitesimal length of ε_δ and ε . Since ε_δ is always much larger than ε of a shock wave, i.e. $\varepsilon_\delta \gg \varepsilon$, there must be $\mu \frac{\Delta u^2}{\varepsilon_\delta} \ll \mu \frac{\Delta u^2}{\varepsilon}$, i.e. the dissipation induced by TS is negligible. Additionally, the flow on the mobile boundary DK is nondissipative. Therefore, Φ in V is mainly contributed by the five shock waves:

$$\Phi = \Phi_{AT} + \Phi_{TB} + \Phi_{BC} + \Phi_{CD} + \Phi_{TG} \quad (5)$$

where Φ_{AT} , Φ_{TB} , Φ_{BC} , Φ_{CD} and Φ_{TG} are the dissipation induced by AT , TB , BC , CD and TG , respectively. Thus, the synergy [28] of these shock waves should make the flow system have the minimal dissipation.

Next we will expound that Φ only depends on the order parameter h_m for a given external parameter θ_w . Since the viscous dissipation is the dominate term of the kinetic energy loss in compressible flows [29, 30], the dissipation ϕ of a oblique shock wave per unit length can be approximate to:

$$\phi \simeq \frac{1}{2} [\rho_a (M_a \mathcal{A}_a \sin \beta)^3 - \rho_b [M_b \mathcal{A}_b \sin(\beta - \theta)]^3] \quad (6)$$

where subscript $\hat{a}\hat{\ddot{Y}}a\hat{a}\hat{\ddot{Z}}$ and $\hat{a}\hat{\ddot{Y}}b\hat{a}\hat{\ddot{Z}}$ denote variables ahead of and behind the shock wave, respectively. θ and \mathcal{A} are the flow deflection angle across the shock wave and the acoustic velocity, respectively. β is the shock angle that satisfies:

$$f_\beta(M_a, \beta, \theta) = 2 \cot \beta \frac{M_a^2 \sin^2 \beta - 1}{M_a^2(\gamma + \cos 2\beta) + 2} - \tan \theta = 0 \quad (7)$$

which means that, for a given Mach number M_a , either of β or θ is known, the other one can be obtained. Furthermore, variables on both sides of a shock front satisfy the classical Rankine-Hugoniot (RH) relations [31–33]:

$$\Omega_b = \Omega_a * X(M_a, \beta) \quad (8)$$

where $\Omega = [M^2, \rho, \mathcal{A}]^T$, $X = [f_M, f_\rho, f_{\mathcal{A}}]^T$ are namely the RH relations, and ‘*’ denotes hadamard product. Therefore, Ω_b and ϕ can be obtained for given Ω_a and θ with (6 - 8). For the straight incident shock wave AT , $\Phi_{AT} = \phi_{AT} \sigma_{AT}$, where σ_{AT} is the length of AT and determined by h_0 , h_m and β_{AT} . ϕ_{AT} can be obtained with θ_w and $\Omega_{AT,a} = [M_0^2, \rho_0, \mathcal{A}_0]^T$. For the Mach stem TG , $\Phi_{TG} = \int_T^G \phi d\sigma$. Since TG is just slightly bend, it can be approximate to a straight one, i.e. $\Phi_{TG} \simeq \frac{1}{2} (\phi_{T(3)} + \phi_G) h_m$, where subscript $\hat{a}\hat{\ddot{Y}}(3)\hat{a}\hat{\ddot{Z}}$ refers to the location near the triple point T in figure 2(a). As $\theta_G = 0$, $\Omega_{a,G} = \Omega_{a,T(3)} = \Omega_{a,AT}$ and $\theta_{T(3)}$ can be calculated by the three-shock theory [34]. Although the Mach stem is moving, its velocity is small compared to the inflow [35]. Therefore, unstable reflections are approximate to quasi steady, which implies (6 - 8) is still available, thus ϕ_G and $\phi_{T(3)}$ can be obtained. For the reflection shock wave TB , $\Phi_{TB} = \phi_{TB} \sigma_{TB}$. stable RR ($h_m = 0$) and stable MR ($h_m = h_{m0} > 0$) correspond to $\beta_{TB} = \beta_{RR}$ and $\beta_{TB} = \beta_{MR}$, respectively, where β_{RR} and β_{MR} can be obtained by the two- and three-shock theory [14, 34], which are shown in figure 2(b). Supposing a transition process of an unstable reflection (UR) from the

stable RR to stable MR, β_{TB} should monotonously decrease from β_{RR} to β_{MR} while h_m monotonously increase from 0 to h_{m0} . Considering the physical reality that the shear layer TS should not touch the reflected surface JK [35] when the stable RR just changes into an UR, β_{TB} must maintain β_{RR} when $h_m = 0 + dh_m$, i.e. $(d\beta_{TB}/dh_m)_0 = 0$. When the UR is near the stable MR with $h_m = h_{m0} \pm dh_m$, β_{TB} is assumed varying linearly, i.e. $(d\beta_{TB}/dh_m)_{h_{m0}} = \text{constant}$. Therefore, β_{TB} can be approximate to:

$$\frac{\beta_{TB} - \beta_{MR}}{\beta_{RR} - \beta_{MR}} = f_{\beta_{TB}}(h_m) = \cos\left(\frac{h_m}{h_{m0}} \cdot \frac{\pi}{2}\right) \quad (9)$$

where function $f_{\beta_{TB}}$ is a phenomenological relation to constrain the variation process of β_{TB} with the order parameter h_m . As β_{TB} can describe the possible unstable state of the system, we call β_{TB} and $f_{\beta_{TB}}$ as ‘the process parameter’ and ‘the process constraint function’, respectively, which are shown in figure 2(c). Then ϕ_{TB} depending on h_m (originally depending on β_{TB}) can be obtained with $\Omega_{TB,a} = \Omega_{AT,b}$. As B is the intersection of TB and the Mach wave RB , σ_{TB} also depends on h_m with geometrical relations. For the shock wave BC , which is curved by the Prandtl-Meyer expansion fan [36, 37], $\Phi_{BC} = \int_B^C \phi_E d\sigma$, where E is the point moving from point B to C . Bai et al [22] has derived the differential relations of β_E and (x_E, y_E) , with which they obtained $\Omega_{E,a}$ and the shape of BC . Based on their theory, we can obtain Φ_{BC} . For shock wave CD , $\Phi_{CD} = \phi_{CD} \sigma_{CD}$. Since $\beta_{CD} = \beta_{CE}$ and $\Omega_{CD,a} = \Omega_{C,a}$, we can obtain both ϕ_{CD} and σ_{CD} . Thus, the total dissipation $\Phi_{CD}(\theta_w, h_m)$ induced by CD can be obtained.

Now we have the total dissipation Φ with formular (5). The synergy principle [28] of shock waves constituting a stable configuration, is that they must make the flow maintain the minimal dissipation. Thus, for a given M_0 , a stable Mach stem h_{m0} should satisfy:

$$\left. \frac{\partial \Phi}{\partial h_m} \right|_{h_{m0}} = 0, \quad \left. \frac{\partial^2 \Phi}{\partial h_m^2} \right|_{h_{m0}} > 0 \quad (10)$$

The landscape of $\Phi(\theta_w, h_m/h_0)$ is shown in figure 3(b) with θ_w varying in the dual-solution domain at $M_0 = 4.5$. As shown in figure 3(a), the initial state is the stable RR corresponding to $\Phi(21^\circ, 0)$, where the possible MR is highly unstable but the RR is stable, which means that a disturbance can not transform the RR to the MR, but can easily transform the MR to the RR. As θ_w increases to 22.5° , a dissipation barrier emerge and two minimal values will be formed corresponding to two stable configurations, i.e. the stable RR and MR at $\Phi(22.5^\circ, 0)$ and $\Phi(22.5^\circ, h_{m0})$, respectively. If θ_w varies continuously and slowly, the disturbance will be not strong enough to transform the RR to the MR, then the configuration maintains the stable RR. It is similar as θ_w increases to 24° , the only difference is that $\Phi(24^\circ, 0) > \Phi(24^\circ, h_{m0})$, but $\Phi(22.5^\circ, 0) < \Phi(22.5^\circ, h_{m0})$. When θ_w increases to 25.5° , the RR becomes unstable, and just a little disturbance can transform it to the MR. Once $\theta_w > 25.5^\circ$, the configuration will stay at the stable MR. As shown in

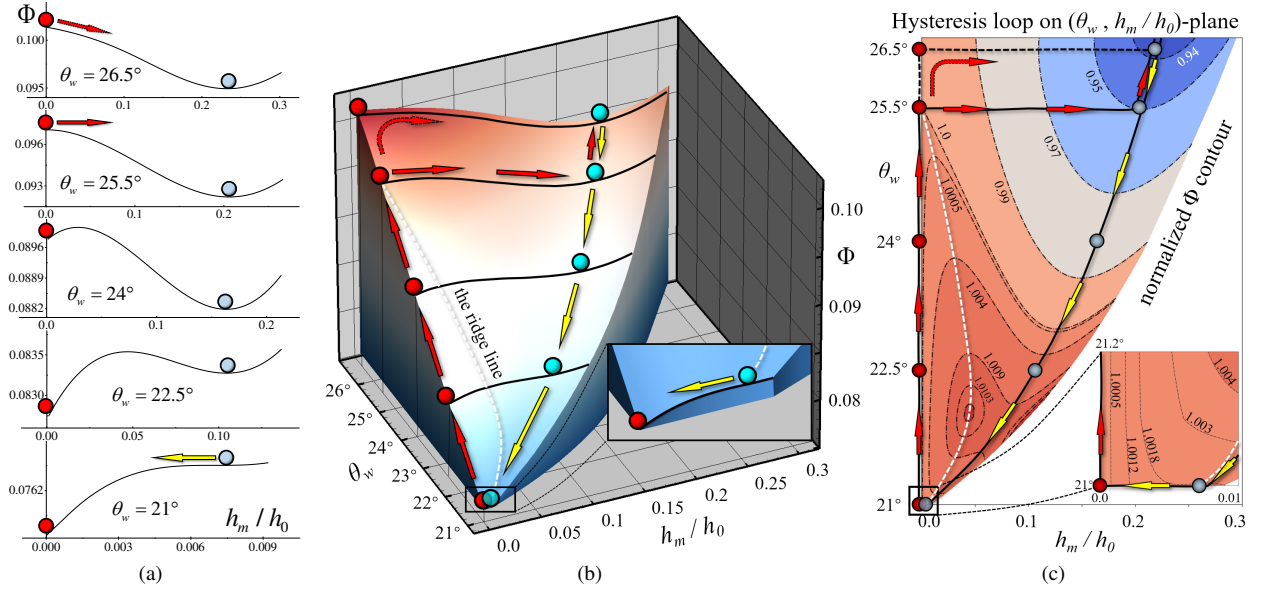


FIG. 3: different perspectives of the total dissipation Φ landscape, where red and blue spheres correspond to stable RRs and MRs, respectively. (a) five latitude lines from the front view of Φ landscape, where Φ versus normalized order parameter h_m/h_0 at $\theta_w = 21^\circ, 22.5^\circ, 24^\circ, 25.5^\circ$ and 26.5° ; (b) the Φ landscape, where red and yellow arrows are the path of $RR \rightarrow MR$ and $RR \leftarrow MR$ in the valley, respectively, and the white dash line is the ridge line; (c) contour of normalized total dissipation $\Phi/\Phi(\theta_w, 0)$, where the black solid line is the hysteresis loop of the $RR \rightleftharpoons MR$ transition, and the black dash line is the path when $\theta_w > 25.5^\circ$.

figure 3(b) and 3(c), the transition point $\theta_w = 25.5^\circ$ is a saddle-node bifurcation of the Φ landscape, i.e. the intersection point of the valley line $\Phi(\theta_w \leq 25.5^\circ, h_m = 0)$ and the ridge line. If θ_w decreases back from 26.5° , although stable RRs are possible theoretically when $\theta_w < 25.5^\circ$, the configuration will always stay at stable MRs until it reaches to 21° , where a little disturbance will transform the MR to the RR. The transition point $\theta_w = 21^\circ$ is another saddle-node bifurcation, i.e. the intersection point of the valley line $\Phi(\theta_w \leq 26.5^\circ, h_m = h_{m0})$ and the ridge line. As θ_w varies from 21° to 26.5° and then back to 21° , a 3D path in the valleys of $\Phi(\theta_w, h_m)$ landscape emerges, which manifests a series of stable configurations. Obviously, the projection of the path to the $(\theta_w, h_m/h_0)$ -plane is the hysteresis loop, as shown in figure 3(c). In addition, it is seen that the $MR \rightarrow RR$ transition occurs very close to $\theta_w^N = 20.92^\circ$, while the $RR \rightarrow MR$ transition takes place at about 25.5° , which is smaller than $\theta_w^D = 26.85^\circ$. This phenomenon, i.e the transition point smaller than θ_w^D , was also observed by Chpoun et al [16], which is clarified now that the MR has a larger stable region than the RR in the dual-solution domain.

Further on, as a validation, we compare h_{m0} obtained by the present theory with previous experimental, numerical and theoretical results, as shown in figure 4. It is seen that, for relatively small $\beta_{AT} < 35^\circ$, the present theory compares remarkably well with experimental [18, 38] and numerical [17] results. For relatively large $\beta_{AT} > 36^\circ$, it follows very well with experimental [38] and numerical [17, 35] results. When $35^\circ < \beta_{AT} < 36^\circ$, it is slightly higher than the experimental [38] and numerical [35] results. In general, the present theory

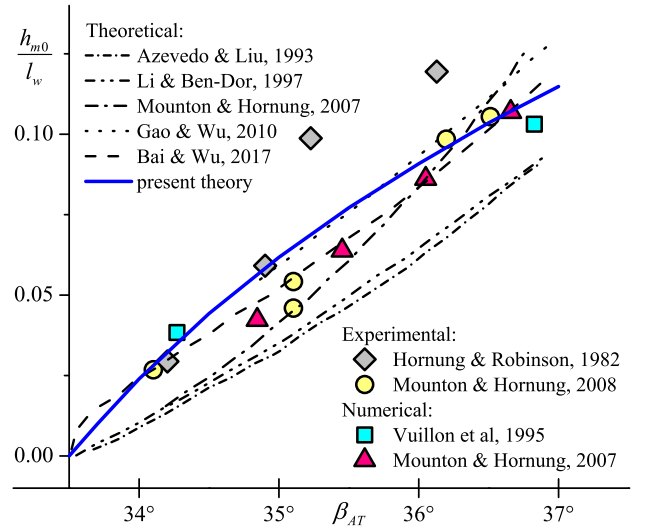


FIG. 4: comparison of the present theory with previous works at $M_0 = 3.98$ and $h_R/l_w \approx 0.4$, including the experimental results from Hornung et al [18, 38], the numerical results from Mouton & Hornung [35] and Vuillon et al [17], and the theoretical results from Azevedo & Liu [39], Li & Ben-Dor[40], Mouton & Hornung [35] and Wu et al [21, 22].

is reasonable and valid.

In this letter, the essence of hysteresis in the shock wave reflection is revealed. Since the dissipation of kinetic energy is demonstrated as the action of the equation governing the

flow field, of which minimal values correspond to steady states of the system, the hysteresis loop is in fact the projection of valley lines in the dissipation landscape, where the saddle-node bifurcations, i.e. intersection points of valley and ridge lines, are actually the transition points. Therefore, the emergence and disappearance evolution of the dissipation barriers, manifested by the ridge line of the dissipation landscape, is the origin of the reflection hysteresis. The present theory, based on the surface geometry of the action, may be generalized to other hysteresis systems.

We are grateful to professor Xin-Liang Li and You-Sheng Zhang for their helpful discussions.

-
- [1] Michael Plischke, Birger Bergersen, Plischke, and Bergersen, *Equilibrium Statistical Physics* (2006).
 - [2] N. Goldenfeld, *Lectures on phase transitions and the renormalization group* (CRC Press, 2018).
 - [3] N. J. Wilkinson, M. A. Alam, J. M. Clayton, R. Evans, H. M. Fretwell, and S. G. Usmar, *Physical Review Letters* **69**, 3535.
 - [4] Q. Xu, I. Sharp, C. Yuan, D. Yi, C. Liao, A. M. Glaeser, A. Minor, J. Beeman, M. C. Ridgway, P. Kluth, *et al.*, *Physical Review Letters* **97**, 155701 (2006).
 - [5] B. Hof, J. Westerweel, T. M. Schneider, and B. Eckhardt, *Nature* **443**, 59.
 - [6] G. Ben-Dov and J. Cohen, *Physical Review Letters* **98**, 064503.
 - [7] K. Avila, D. Moxey, A. de Lozar, M. Avila, D. Barkley, and B. Hof, *Science* **333**, 192.
 - [8] G. Lemoult, L. Shi, K. Avila, S. V. Jalikop, M. Avila, and B. Hof, *Nature Physics*.
 - [9] Mueller and E. J., *Physical Review A* **66**, 063603.
 - [10] D. Diakonov, L. Jensen, C. J. Pethick, and H. Smith, *Physical Review A* **66**, 013604 (2002).
 - [11] O. Morsch and M. Oberthaler, *Reviews of Modern Physics* **78**, 179.
 - [12] S. Eckel, J. G. Lee, F. Jendrzejewski, N. Murray, C. W. Clark, C. J. Lobb, W. D. Phillips, M. Edwards, and G. K. Campbell, *Nature* **506**, 200.
 - [13] E. Mach, *Sitzungsbr. Akad. Wiss. Wien* **78**, 819 (1878).
 - [14] J. von Neumann, Bureau of Ordinance, Explosives Research Report (1943).
 - [15] H. G. Hornung, H. Oertel, and R. J. Sandeman, *Journal of Fluid Mechanics* **90**, 541 (1979).
 - [16] A. Chpoun, D. Passerel, H. Li, and G. Ben-Dor, *Journal of Fluid Mechanics* **301**, 19 (1995).
 - [17] J. Vuillon, D. Zeitoun, and G. Ben-Dor, *Journal of Fluid Mechanics* **301**, 37 (1995).
 - [18] H. Hornung and M. Robinson, *Journal of Fluid Mechanics* **123**, 155 (1982).
 - [19] M. Ivanov, S. Gimelshein, and A. Beylich, *Physics of Fluids* **7**, 685 (1995).
 - [20] G. Ben-Dor and G. Ben-Dor, *Shock wave reflection phenomena*, Vol. 2 (Springer, 2007).
 - [21] B. Gao and Z. Wu, *Journal of Fluid Mechanics* **656**, 29 (2010).
 - [22] C.-Y. Bai and Z.-N. Wu, *Journal of Fluid Mechanics* **818**, 116 (2017).
 - [23] H. v. Helmholtz, *Wiss. Abh* **1**, 223 (1868).
 - [24] L. Rayleigh, *The London, Edinburgh, and Dublin Philosophical Magazine and Journal of Science* **26**, 776 (1913).
 - [25] J. Serrin, in *Fluid Dynamics I/Strömungsmechanik I* (Springer, 1959) pp. 125–263.
 - [26] K. Ho, D. Yang, and J. Wu, *Journal of Engineering and Thermophysics* **9**, 10 (1988).
 - [27] J.-Z. Wu, H.-Y. Ma, and M.-D. Zhou, *Vorticity and vortex dynamics* (Springer Science & Business Media, 2007).
 - [28] H. Haken, *Physics Bulletin* **28**, 412 (1977).
 - [29] S. E. Guarini, R. D. Moser, K. Shariff, and A. Wray, *Journal of Fluid Mechanics* **414**, 1 (2000).
 - [30] S. Pirozzoli, F. Grasso, and T. Gatski, *Physics of fluids* **16**, 530 (2004).
 - [31] W. J. M. Rankine, *Philosophical Transactions of the Royal Society of London*, 277 (1870).
 - [32] P. Rankine, *Journal de l'École Polytechnique. Paris* **57**, 3 (1887).
 - [33] M. D. Salas, *Shock waves* **16**, 477 (2007).
 - [34] J. Von Neumann, NAVORD Rep. 203-45 (1945).
 - [35] C. A. Mouton and H. G. Hornung, *Aiaa Journal* **45**, 1977 (2007).
 - [36] R. Courant and K. O. Friedrichs, *Supersonic flow and shock waves*, Vol. 21 (Springer Science & Business Media, 1999).
 - [37] R. Von Mises, H. Geiringer, and G. S. S. Ludford, *Mathematical theory of compressible fluid flow* (Courier Corporation, 2004).
 - [38] C. A. Mouton and H. G. Hornung, *Physics of Fluids* **20**, 541 (2008).
 - [39] D. J. Azevedo and C. S. Liu, **31**, 83 (1993).
 - [40] H. Li and G. Ben-Dor, *Journal of Fluid Mechanics* **341**, 101 (1997).